UNCLASSIFIED
SECURITY CLASSIFICATION OF THIS PAGE

(2)

AD-A211 124 JMENTATION PAGE

Form Approved
OMB No. 0704-0188

1a. REPORT SECURITY CLASSIFICATION UNCLASSIFIED	1b. RESTRICTIVE MARKINGS
2a. SECURITY CLASSIFICATION AUTHORITY	3. DISTRIBUTION/AVAILABILITY OF REPORT DISTRIBUTION UNLIMITED
2b. DECLASSIFICATION/DOWNGRADING SCHEDULE	
4. PERFORMING ORGANIZATION REPORT NUMBER(S) FJSRL-JR-87-0012	5. MONITORING ORGANIZATION REPORT NUMBER(S)
6a. NAME OF PERFORMING ORGANIZATION Frank J. Seiler Research Lab 6b. OFFICE SYMBOL (If applicable) FJSRL/NC	7a. NAME OF MONITORING ORGANIZATION
6c. ADDRESS (City, State, and ZIP Code) USAF Academy Colorado 80840-6528	7b. ADDRESS (City, State, and ZIP Code)
8a. NAME OF FUNDING/SPONSORING ORGANIZATION AF Office of Scientific Research 8b. OFFICE SYMBOL (If applicable) AFOSR	9. PROCUREMENT INSTRUMENT IDENTIFICATION NUMBER
8c. ADDRESS (City, State, and ZIP Code) Bldg 410 Bolling AFB, DC 20332	10. SOURCE OF FUNDING NUMBERS PROGRAM ELEMENT NO.: PE61101F PROJECT NO.: 2303 TASK NO.: F2 WORK UNIT ACCESSION NO.: 10
11. TITLE (Include Security Classification) Nuclear Magnetic Resonance in Molten Salts	
12. PERSONAL AUTHOR(S) John S. Wilkes	
13a. TYPE OF REPORT Journal Article 13b. TIME COVERED FROM _____ TO _____	14. DATE OF REPORT (Year, Month, Day) 87 15. PAGE COUNT 20
16. SUPPLEMENTARY NOTATION	
17. COSATI CODES FIELD / GROUP / SUB-GROUP	18. SUBJECT TERMS (Continue on reverse if necessary and identify by block number) Thallium 205

19. ABSTRACT (Continue on reverse if necessary and identify by block number)

Nuclear magnetic resonance (NMR) spectroscopy provides information about the structure of molten salts and about interactions among molten salt components. This contribution reviews the application of NMR spectroscopy to molten salts done in this laboratory and by others. The fundamentals of the NMR method are presented, with emphasis on aspects particularly useful to molten salt samples. The limitations to the method resulting from the nature of molten salts and nuclei encountered are discussed. Examples of the types of information about molten salts provided by NMR experiments that are useful to chemists are presented. Chloroaluminate molten salts are the primary melt system used to illustrate the usefulness of NMR spectroscopy. Experiments in organic melts and the use of ^{205}Tl as a probe in nitrates and halides are also treated. Reprints. (AW)

20. DISTRIBUTION/AVAILABILITY OF ABSTRACT ☒ UNCLASSIFIED/UNLIMITED ☐ SAME AS RPT ☐ DTIC USERS	21. ABSTRACT SECURITY CLASSIFICATION UNCLASSIFIED
22a. NAME OF RESPONSIBLE INDIVIDUAL JOHN S. WILKES	22b. TELEPHONE (Include Area Code) (719)472-2655 22c. OFFICE SYMBOL FJSRL/NC

DD Form 1473, JUN 86 *Previous editions are obsolete.* SECURITY CLASSIFICATION OF THIS PAGE

UNCLASSIFIED

NUCLEAR MAGNETIC RESONANCE IN MOLTEN SALTS

John S. Wilkes
The Frank J. Seiler Research Laboratory
United States Air Force Academy
Colorado Springs, CO 80840
USA

ABSTRACT. Nuclear magnetic resonance (NMR) spectroscopy provides information about the structure of molten salts and about interactions among molten salt components. This contribution reviews the application of NMR spectroscopy to molten salts done in this laboratory and by others. The fundamentals of the NMR method are presented, with emphasis on aspects particularly useful to molten salt samples. The limitations to the method resulting from the nature of molten salts and nuclei encountered are discussed. Examples of the types of information about molten salts provided by NMR experiments that are useful to chemists are presented. Chloroaluminate molten salts are the primary melt system used to illustrate the usefulness of NMR spectroscopy. Experiments in organic melts and the use of ^{205}Tl as a probe in nitrates and halides are also treated.

1. INTRODUCTION TO THE NMR METHOD

1.1 CW and FT NMR Spectroscopy

The electromagnetic spectrum spans from acoustic frequencies at the low end to gamma ray frequencies at the high end. In chemistry the range from radio frequencies (about 3×10^6 Hz) to ultraviolet frequencies (3×10^{16} Hz) has been found to be useful. The high energy irradiation available in the ultraviolet provides information about electronic transitions, infrared spectroscopy excites bond vibrations and microwave frequencies are at the energy for rotations and electron spin transitions. Atomic nuclei in a magnetic field will absorb energy in the radio frequency portion of the spectrum. This last phenomenon provides the basis of nuclear magnetic resonance (NMR) spectroscopy, which is a common analytical tool available in most chemical laboratories.

The fundamental basis of the NMR effect is simple if one uses the simplest of concepts for the atomic nucleus: the spinning charged sphere. In reality, the nucleus is an inhabitant of a world where quantum mechanics governs, so a rigorous explanation of NMR is

G. Mamantov and R. Marassi (eds.), Molten Salt Chemistry, 217–236

rather non-intuitive and the arguments can get mathematically abstruse. In this introduction the basic principles of NMR will be outlined and the features of the spectroscopy that provide useful information to molten salt chemists will be presented. This should in no way be considered a complete treatment of NMR principles, but rather a familiarization of the nomenclature and an exposure to the features that reveal chemical information. There are many good texts that provide comprehensive treatments of the material outlined here (1,2).

A spinning charged sphere is a magnetic dipole. In the presence of a magnetic field this magnetic dipole will precess about its spin axis, much like a spinning top in a gravitational field. This precession may be visualized like a mechanical top or, more usefully, as a vector revolving about an axis parallel with the external magnetic field. The length of the vector is the magnetic moment of the nucleus. The "vector representation" of the nucleus will be used here, since it provides the clearest way to understand the interaction of radio frequency radiation with the nucleus.

In a magnetic field of a given strength a nucleus of spin 1/2 can orient in two states. Nuclei with spin other than 1/2 will have more orientations, but for the sake of simplicity the treatment that follows will consider only 1/2 spins. The energy difference between the two orientations is quantized and is proportional to the field strength. It happens that the energy required for the transition corresponds to radio frequencies. The simplest NMR spectrometer would thus consist of a magnet with a sample containing atomic nuclei (i.e., *matter*) *between* its poles, a radio frequency transmitter, and a radio receiver to detect the absorption of energy. This would be a CW (continuous wave) spectrometer, and a recording from the receiver as the transmitter frequency was swept would be an NMR spectrum. In the vector representation of NMR the term resonance refers to the condition when the magnetic vector from the incident radiation is perpendicular to the applied magnetic field (B_0) and is rotating about B_0 at the same rate that the nucleus is precessing. This is called the Larmor frequency, ν, given by

$$\nu = |\gamma/2\pi| B_0 \qquad (1)$$

where γ is the gyromagnetic ratio of the nucleus. To the first order and in the grossest sense, the NMR spectrum depends on one property of the nucleus (γ) and two external forces (from ν and B_0).

For reasons that will be discussed later, not every nucleus with the same γ will resonate at the same frequency, so as the CW spectrometer sweeps in frequency, many resonance lines may be observed. The signal/noise may be improved by collecting information about the nuclear resonance frequencies in the time domain with an FT (Fourier transform) spectrometer. The FT instrument provides a short pulse of radio frequency energy. As the nuclei make their transitions a signal is induced in a receiver that decays with time. The signal, called the FID (free induction decay), contains information about low frequency resonances at early times and higher frequencies at longer times. A Fourier transform of the FID (plus some phase information)

produces a frequency domain spectrum similar to that from a CW instrument, but having used a "sweep" lasting about a second. The maximum intensity of the FID occurs when a 90° pulse is used. That is, the pulse time is precisely long enough to rotate the magnetization vector 90° from its position at equilibrium in the rotating frame of reference. If the pulse rotates the magnetization vector 180°, then no FID is observed, since the decay is along the z-magnetization axis.

1.2 Relaxation Processes

Observation of the NMR phenomenon requires that a reasonable portion of the population of nuclei be in the lower energy state at the beginning. Unlike most electronic transitions, nuclear transitions to the equilibrium state seldom occur spontaneously. They require interactions with external fluctuating fields of the appropriate frequency. This process of interaction with the environment is called relaxation. Study of the nuclear relaxation can provide useful information about the surroundings of the nucleus, i.e., molecules and such. Relaxation times are denoted T_1 and T_2 (spin-lattice and spin-spin), which specify the fundamental relaxation mechanisms. Frequently relaxation rates ($1/T_1$ and $1/T_2$) are used instead of relaxation times.

For spin 1/2 nuclei T_1 relaxation is the most important. There are many mechanisms for T_1 relaxation, the details of which need not be discussed here. The measurement of T_1 is of interest, since discussion of some relaxation experiments in molten salts occurs later in this report. T_1 relaxation of a nucleus to the equilibrium state occurs exponentially with time. One need only measure the fraction of nuclei that are still in the non-equilibrium state as a function of time. The slope of a $\ln(N_\infty - N_t)$ vs time (where N_∞ and N_t are the fractions magnetized at time=∞ and time=t) will yield T_1. N_∞ and N_t may be easily measured by a simple sequence of pulses on a FT spectrometer. A 180° pulse is applied, then after a waiting period t a 90° pulse is applied. The second pulse "samples" the magnetization remaining after time=t, which is reflected in the signal intensity (after transformation). This technique is called the spin inversion recovery method.

1.3 Chemical Shift

If Equation 1 were the sole determinant of the resonant frequency, then NMR would be of little interest to chemists. Fortunately, the Larmor frequency of a nucleus is affected by numerous features of its environment. The effect of the local magnetic environment may be interpreted in terms of molecular or ionic structure, bonding, and interactions in general.

The chemical shift is actually a rather minor contributor to the ultimate resonant frequency, but it is the one that provides the most useful information. Local perturbations to the applied magnetic field are usually divided into diamagnetic contributions (including chemical

shifts) and paramagnetic contributions (which are usually quite large). Sometimes paramagnetic effects completely mask any effect of chemical shift, such as when conduction electrons are present from metals (the Knight shift). Also, the bulk susceptibility of the medium can greatly affect the resonant frequency. Fortunately, shifts are usually measured against reference materials that are equally affected by the medium.

The source of the chemical shift is electronic shielding. The simplest example of electronic shielding comes from the circulation of s electrons about a nucleus. This generates a local field that opposes the applied field, thus changing the resonant frequency. The local field at atom i will be modified a small amount denoted by the shielding constant, σ_i. Equation 1 becomes

$$\nu_i = |\gamma/2\pi| B_o(1 - \sigma_i) \tag{2}$$

The chemical shift, denoted δ, is expressed in terms of difference of ν_i from the ν of a reference substance. Since the shielding effect is so small, a factor of 10^6 is applied, and the chemical shift in Equation 3 is in parts per million (ppm).

$$\delta = 10^6(\nu_{sample} - \nu_{ref.})/\nu_{ref.} \text{ at constant } B_o \tag{3}$$

The quantity $(\nu_{sample} - \nu_{ref.})$ generally spans the range of 10^{-1} to 10^3 Hz out of a spectrometer frequency of $\sim 10^7$ Hz.

The paramagnetic contribution to chemical shifts has been described in a general theory of magnetic shielding by Ramsey, and results in Equation 4.

$$\delta_p = -\frac{16}{3}\mu_B^2 \left\langle \frac{1}{r^2} \right\rangle \frac{B}{\Delta E} \tag{4}$$

The interesting term in Equation 4 is B. It basically contains information about the interaction of the nucleus with its surroundings. It depends on the coordination number and the orbital overlaps, and is usually interpreted as an indicator of degree of covalency.

1.4 Chemically Exchanging Systems

The frequency of the electromagnetic radiation used in NMR is low compared to that used in most other spectroscopies. In many cases interactions among species containing the nuclei under observation are occurring faster than the time scale defined by the NMR frequency. That case, called the fast exchange limit, is much like photographing a fast event with a camera having a slow shutter speed. An averaged or blurred image results. Valuable information about dynamic processes may be gained from the proper interpretation of the NMR behavior of these systems.

There are three cases that can occur in the NMR of exchanging systems. First, the exchange rate may be slow relative to the

difference in chemical shifts of the two (or more) exchanging species. This is the slow exchange limit, and one simply sees the resonances of the separate species. If the exchange rate is very fast relative to the difference in chemical shifts of the exchanging species (the fast exchange limit), then only a single line is observed. The observed shift or frequency is intermediate between those of the exchanging species, and is determined by the relative populations of the species. For A and B in fast equilibrium the observed shift (δ_{obs}) is given by Equation 5,

$$\delta_{obs} = X_A\delta_A + X_B\delta_B \tag{5}$$

where X_A and X_B are the mole fractions of A and B at equilibrium.

At intermediate rates the analysis of the NMR lines is a little more difficult. The spectrum may range from two partially merged and broadened peaks to a single broadened peak. The line shape is described by the Bloch equations, which basically say that the shape is proportional to the exchange rate divided by the frequency (or shift) difference between the species. Line shape simulations using the function $g(\nu)$ in Equation 6 (for two site exchange) are often used to obtain exchange rates from NMR data.

$$g(\nu) = K\frac{\tau(\nu_A-\nu_B)^2}{[\frac{1}{2}(\nu_A+\nu_B)-\nu]^2 + 4\pi^2\tau^2(\nu_A-\nu)^2(\nu_B-\nu)^2} \tag{6}$$

The quantity K is a normalization constant, τ is the exchange lifetime and ν_A and ν_B are the resonance frequencies of species A and B.

2. PRACTICAL CONSTRAINTS

2.1 Receptivity

In order to observe the NMR spectrum of a nucleus in a chemically interesting situation, there must be sufficient signal from the spectrometer. The intensity of the NMR response varies over many orders of magnitude for different nuclei. A useful figure of merit for NMR response is the receptivity. The receptivity depends on the gyromagnetic ratio of the nucleus and the abundance of the nucleus. It is defined as γ^3C, where γ is the magnetogyric ratio and C is the natural abundance of the nuclide.

The receptivity relative to a familiar nucleus, such as ^1H (D^H) or ^{13}C (D^C) , is the number most often used to gauge the ease of observation of an unfamiliar nucleus. A relative receptivity near that of ^1H insures that a strong signal will be available (other things being equal). A relative receptivity near that of ^{13}C will require many FID accumulations over a considerably longer period of time. For example, NMR of ^{15}N ($D^C = 2.19 \times 10^{-2}$) is difficult to do, while ^{205}Tl ($D^C = 7.91 \times 10^2$) is relatively easy. Relative receptivities are listed in many textbooks and handbooks.

2.2 Quadrupolar Nuclei

Many nuclei do not have 1/2 spins. Those that do not are called quadrupolar nuclei, and are more complex in their NMR behavior. The source of the complexity is that the nuclei may have more than two states in a magnetic field. This provides for a significant contribution to the T_2 relaxation time. The end result is that the NMR spectra of quadrupolar nuclei can have broad lines, often many thousands of Hz wide. If the spectrometer frequency is low and there is an efficient exchange mechanism operating, then the nucleus may be unobservable. ^{27}Al is a quadrupolar nucleus and is the predominately abundant isotope. NMR spectroscopy in molten chloroaluminates must deal with the quadrupolar effects.

The quadrupolar exchange rate ($1/T_{2Q}$) determines the line width, and is shown in Equation 7.

$$\frac{1}{T_{2Q}} = \frac{3\pi^2}{10} \frac{2I+3}{I^2(2I+1)} \left(1 + \frac{\eta_a^2}{3}\right) \frac{(e^2Qq)^2}{h} \tau_c \qquad (7)$$

The linewidth will depend principally on two properties of the nucleus (I, the spin and Q, the quadrupole moment) and two features of the environment (η_a, an asymmetry factor of the surrounding electronic field and τ_c, the correlation time).

2.3 Magnetic Field

The nature of the magnetic field has a substantial effect on the quality of the NMR data obtained and the amount of useful information that may be gained from the spectrum. The three important properties of the field are strength, homogeneity and stability. The resonance frequency of a nucleus is directly proportional to the field strength. An increase in strength has the principal benefit of improving resolution. Commercial NMR spectrometers have magnets capable of fields between 1.5 and 12 T. Field strengths above about 2 T are provided by superconducting magnets. Homogeneity of the field is extremely important due to the very small shifts that are usually observed relative to the applied frequency. Homogeneity greater than 1 part in 2×10^8 is necessary. Stability over long periods of time is required for long duration data acquisition. This is not difficult to do if the field/frequency is locked onto a reference resonance. Stability of greater than 1 part in 1×10^9/hr is necessary.

2.4 Temperature

Temperature does not have a major effect on the NMR phenomenon per se. Temperature does have a number of ancillary effects that affect the NMR data greatly. Most molten salts are liquid at relatively high temperatures, so it is common to have to contend with temperature effects in the study of molten salts by NMR.

The stability of the materials used to construct the probe at high temperature is a major concern. Commercial probes can withstand temperatures up to about 200° C. For temperatures above this, probes are usually custom made.

Temperatures significantly different from the magnet temperature affects the field homogeneity. A high temperature probe must compensate for this effect.

Finally, high temperature can greatly change properties of the sample that in turn affect the NMR behavior. Correlation times are sensitive to absolute viscosity of the sample, which is dependent on temperature. The line shape is sensitive to exchange rate, which is also a function of temperature. Temperature effects on the integrity of the sample, such as vapor pressure and thermal decomposition must be considered when performing NMR experiments at high temperature.

3. CHEMICAL INFORMATION FROM NMR

NMR spectroscopy has been applied to many different classes of molten salts and has provided several types of information about molten salts. This review will concentrate on NMR spectroscopy applied to chloroaluminate melts. The application of NMR to chloroaluminates has some practical advantages, but the primary reason for its emphasis here is that low melting chloroaluminate melts are the principal research interest of the author. Some organic halide melts, inorganic halides and nitrates will also be used to illustrate the usefulness of the NMR method in molten salt chemistry.

The types of information provided by NMR spectroscopy about molten salts fall into three categories: speciation, interactions and complexation. The NMR data required to provide that information are from chemical shifts, line shape analysis, modeling of exchanging nuclei and analysis of relaxation times.

3.1 Chloroaluminates

As a class of molten salt, chloroaluminates consist of aluminum chloride and some chloride donor. The chloride donor may be an organic chloride salt, in which case the resulting melts often have extraordinarily low melting points. Two such organic chloride salts have been used in recent years: 1-(1-butyl)pyridinium chloride (BuPyCl), which results in a 1-(1-butyl)pyridinium cation ($BuPy^+$) in the melt and 1-methyl-3-ethylimidazolium chloride (MeEtImCl) which results in a 1-methyl-3-ethylimidazolium cation ($MeEtIm^+$) in the melt. More details about these molten salts are presented by other authors participating in this Study Institute.

3.1.1 Speciation. The interpretation of NMR data in terms of species is built around the chloroaluminate electrolyte model. That model is a group of equilibria among chloroaluminate anions and $AlCl_3$:

$$2AlCl_3 \rightleftharpoons Al_2Cl_6$$

$$Cl^- + AlCl_3 \rightleftharpoons AlCl_4^-$$

$$AlCl_4^- + AlCl_3 \rightleftharpoons Al_2Cl_7^-$$

$$Al_2Cl_7^- + AlCl_3 \rightleftharpoons Al_3Cl_{10}^-$$

The model predicts that as the composition of the binary melt becomes richer in $AlCl_3$ the anions present will change smoothly from Cl^- to $AlCl_4^-$ to $Al_2Cl_7^-$ as shown in figure 1. ($Al_3Cl_{10}^-$ is not shown in the figure.)

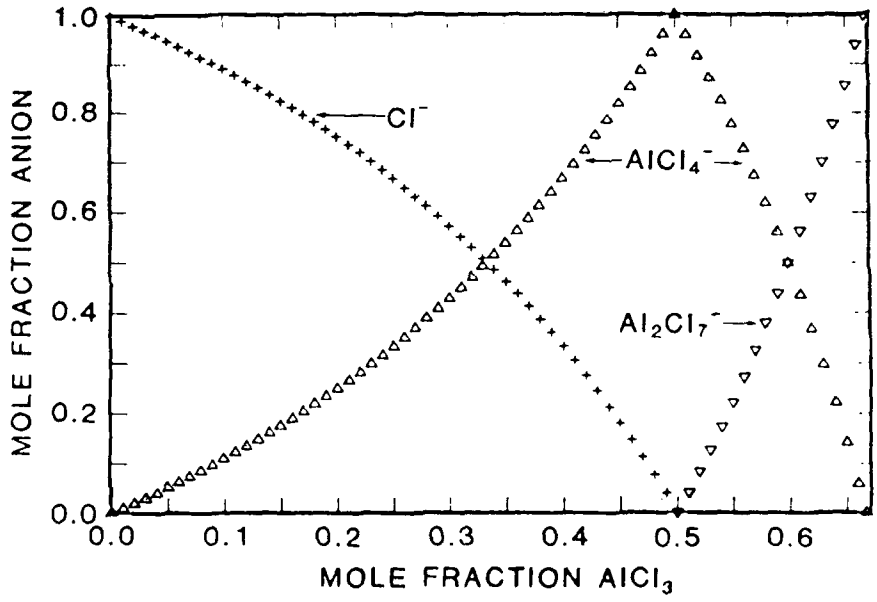

Figure 1. Chloroaluminate Anions.

NMR of ^{27}Al in $AlCl_3$-BuPyCl melts was first reported by Gray and Maciel (3). They observed a single sharp line in basic melts ($AlCl_3$ < BuPyCl) and a single broad line in acidic melts ($AlCl_3$ > BuPyCl).

They were able to partially resolve two components of the broad lines in an acidic melt by raising the temperature (thus reducing viscosity) and by suppressing the acquisition of low frequency data from the FID with an extraordinarily long preacquisition delay time. The partially resolved two line spectrum was presumably due to a narrow line contribution by $AlCl_4^-$ and a broad line contribution from $Al_2Cl_7^-$. They calculated a simulated spectrum that closely matched the observed one, but the fractions of the two components were meaningless due to the suppression of the broad line intensity.

We performed a more extensive series of ^{27}Al NMR experiments in $AlCl_3$-MeEtImCl melts (4). With a relatively low field spectrometer we also observed a single broad line in acidic melt samples. The trick of using a long preacquisition delay time partially resolved the spectrum into two lines, one narrow and one broad as seen in figure 2.

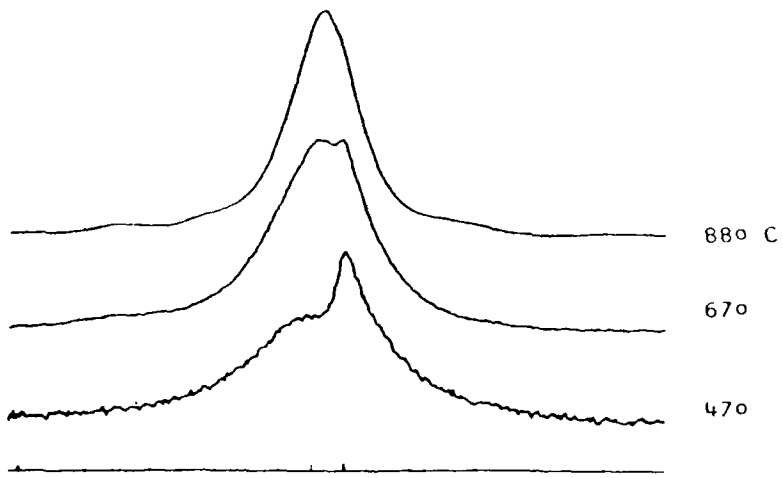

Figure 2. ^{27}Al NMR spectra in $AlCl_3$-MeEtImCl melts. Melt composition is 0.60 mole fraction $AlCl_3$.

The two site exchange simulations shown in figure 3 reproduce the experimental spectra quite well. Like the earlier work, we interpreted the narrow line as evidence for the $AlCl_4^-$ species and the broad line as the $Al_2Cl_7^-$ species.

The linewidth of the ^{27}Al resonance varied from 140 Hz for a slightly acidic composition (0.5073 mole fraction $AlCl_3$, "N") to 2170 Hz for a strongly acidic composition (N=0.525). This is to be expected in light of Equation 7. The situation is complicated by the fact that the species containing the quadrupolar ^{27}Al and the viscosity are both changing as a function of composition. The change in species affects the η_a term in Equation 7 while viscosity controls the correlation time (τ_c). The absolute viscosities of the melts are

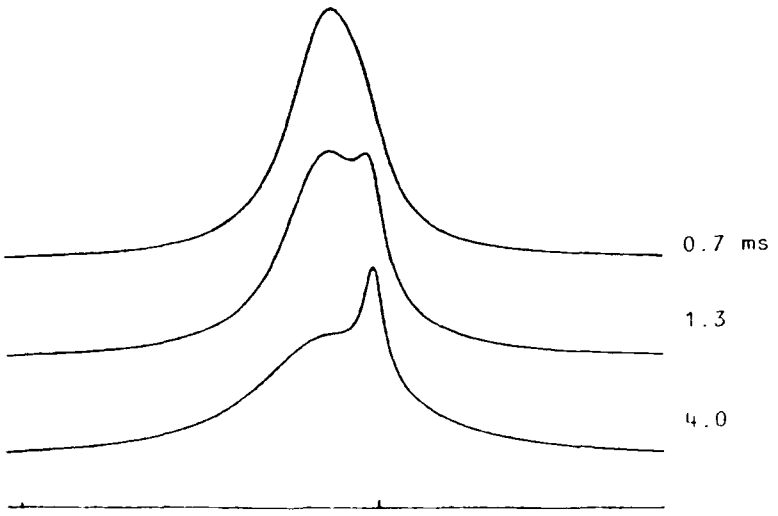

Figure 3. Two site exchange simulation of spectra from figure 3.

known as a function of temperature and composition, so the effect of viscosity may be corrected (τ_c is directly proportional to absolute viscosity). Figure 4 shows the linewidths corrected for viscosity plotted as a function of composition. The composition axis in figure 4 is a little unusual. The use of mole fraction $AlCl_4^-$ provides an axis linear in an anion common to both basic and acidic melts. Note that in very acidic compositions ($AlCl_4^-$ mole fraction > 0.7) the widths deviate from the regular trend up to that point. This may indicate the presence of a new exchanging species in very acidic melts.

The exchange lifetimes (τ) that were entered into the line shape algorithm are listed in figure 3. A rough activation energy for the exchange process may be determined from the exchange rate ($1/\tau$) dependence on temperature. The value is 10 kcal/mol, which is asgreement with the value of 13 kcal/mol obtained by MNDO calculation (5) for the process :

$$Al^*Cl_4^- + Al_2Cl_7^- \rightleftharpoons Al^*AlCl_7^- + AlCl_4^-$$

If there is a third exchanging species then the τ values obtained for two site exchange should be viewed with suspicion.

Further support for the chloroaluminate electrolyte model comes from ^{27}Al spin-lattice relaxation rate studies in $AlCl_3$-BuPyCl melts performed by Matsumoto and Ichikawa (6). These workers observe normal single exponential T_1 decay rates for all basic melts and for melts having the composition N = 0.5 and 0.67. At all other acidic

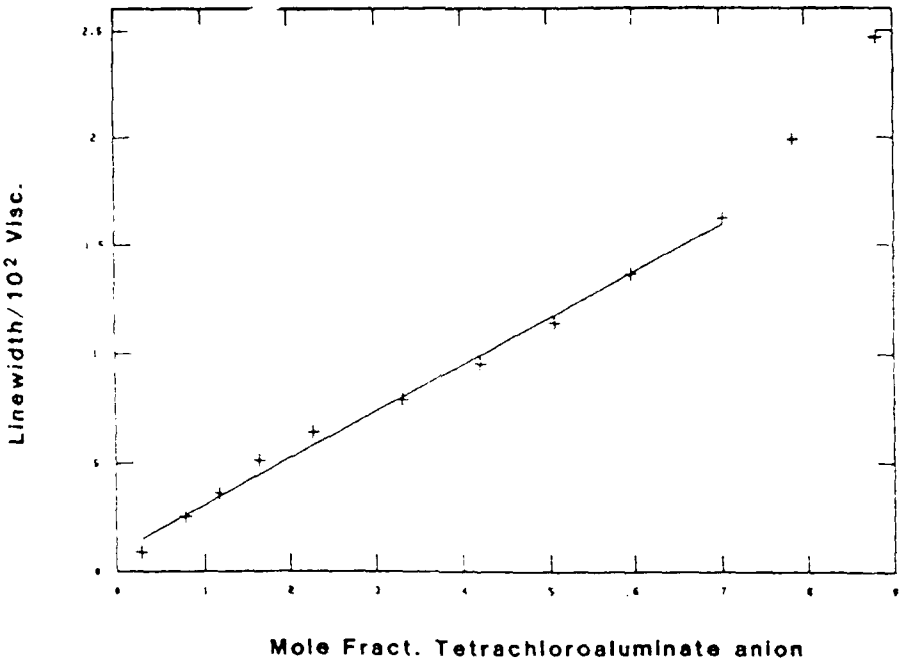

Figure 4. ^{27}Al NMR linewidths corrected for viscosity vs composition

compositions the inversion recovery curves appear to be combinations of at least two exponential decays. The authors interpret these results as arising from the presence of two species relaxing at different rates. By curve fitting they were able to estimate the relative populations of the different relaxing species. The result was a figure that looks much like figure 1. One very interesting feature of their study was that they measured the relaxation rates in melts up to 0.79 mole fraction $AlCl_3$. In these very acidic melts they claim to see $Al_3Cl_{10}^-$ and Al_2Cl_6.

In the ^{27}Al studies described so far the presence of two contributors to the broad line in acidic melts has been inferred from line shape analysis, relaxation rates or revealed by discarding data from the broad component of the FID. We have taken ^{27}Al NMR spectra of $AlCl_3$-MeEtImCl melts at very high field in an attempt to separate the lines (7). Figure 5 shows the ^{27}Al spectra at different compositions run in a 500 MHz spectrometer. The basic and neutral melts show only a single sharp line attributable to $AlCl_4^-$, as seen in low field spectra. In acidic melts, what was a single line at low field is now resolved into separate lines. As the melt is made

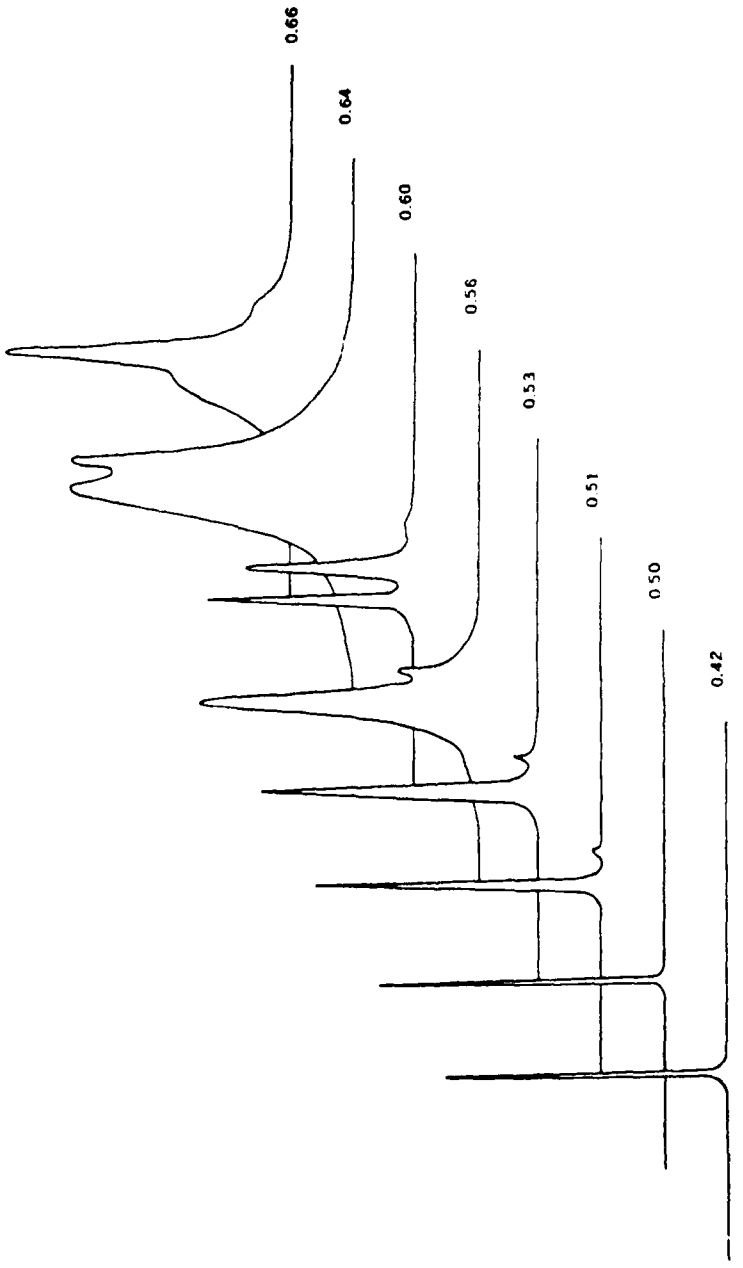

Figure 5. High field ^{27}Al NMR spectra of $AlCl_3$-MeEtImCl melts at 80° C.

slightly acidic a additional well resolved line appears due to $Al_2Cl_7^-$. At very acidic compositions a third species is clearly present, probably due to $Al_3Cl_{10}^-$.

^{35}Cl and ^{37}Cl NMR experiments have been attempted in the $AlCl_3$-MeEtImCl melts without success (8). Both isotopes are quadrupolar, the resonant frequencies for both are rather low, and there are undoubtedly numerous efficient exchange mechanisms. All of those factors contribute to an impossibly broadened signal.

3.1.2 Interactions. The organic cation in the $AlCl_3$-BuPyCl and $AlCl_3$-MeEtImCl melts may be seen easily by ^1H and ^{13}C NMR spectroscopy. The first such observations were by Osteryoung and coworkers in the $AlCl_3$-BuPyCl system (9). They compared the ^1H and ^{13}C chemical shifts of nuclei in the $BuPy^+$ ion in acidic chloroaluminate and bromoaluminate melts and concluded that there was no extensive ion pairing. They also studied the effect of addition of benzene to the melt and found that the solvent promoted ion-ion interactions. Osteryoung et al. did not report any results for basic melts, where the effect of composition was later found to be more pronounced.

We have done many ^1H and ^{13}C NMR experiments, primarily in the $AlCl_3$-MeEtImCl melts, in an attempt to understand anion-cation interactions. Figure 6 shows the results of an early experiment that revealed the pronounced difference in the composition dependence of proton chemical shifts between the basic and acidic melts. The signals are sharp and the change in chemical shift in the basic compositions suggests that the chemical shifts are determined by more than one species at the fast exchange limit. The most likely explanation is that the $MeEtIm^+$ ion exchanges among environments that are magnetically distinct and are defined by the nearest neighbor anions to the cations being observed. A relationship like Equation 5 (for two site exchange) or similar (for more than two sites) would apply.

A more detailed analysis of the dependence of chemical shift on melt composition reveals that there are more than two environments for the cation. For basic melts, three magnetically distinct environments may be visualized arising from two nearest neighbor anions that could be both Cl^-, both $AlCl_4^-$ or one of each. Those situations are depicted in figure 7. These species in figure 7 need not be discrete but may be envisaged as portions of oligomeric chains of alternating cations and anions. Simple ion pairs, as suggested by Taullele and Popov (10), are not sufficient to explain the data. The chemical shift resulting from exchange among three environments as in figure 7 is given by

$$\delta_{obs} = \delta_2 Y_1^2 + \delta_{52} Y_1 Y_4 + \delta_8 Y_4^2 \qquad (7)$$

The subscripts associated with each δ denote the magnetic environment for the cation containing the nucleus under observation (vide infra) and Y_1 and Y_4 are ion fraction of Cl^- and $AlCl_4^-$.

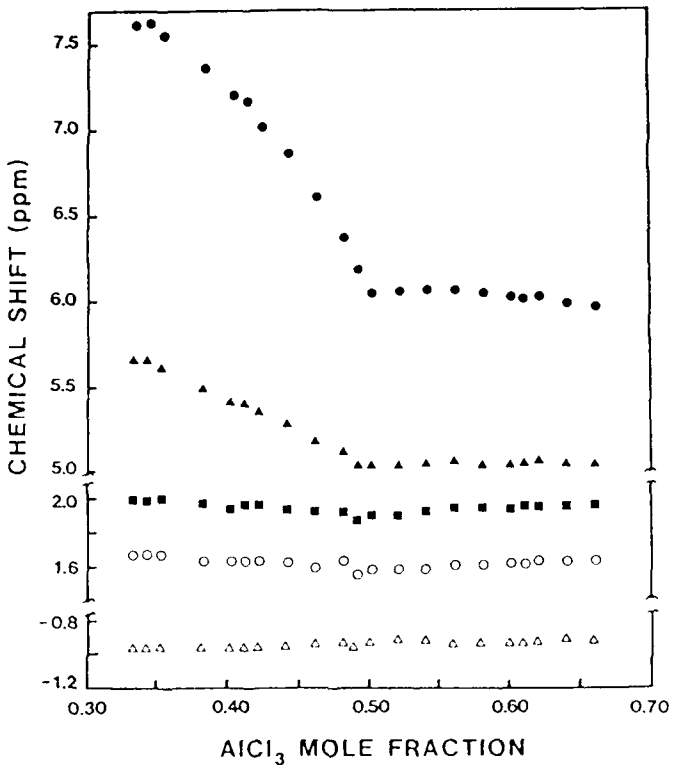

Figure 6. Proton chemical shifts in $AlCl_3$-MeEtImCl melts. From top to bottom the data are for H-2 (proton at ring position 2), H-4&5, N-CH_2, N-CH_3, and CH_3.

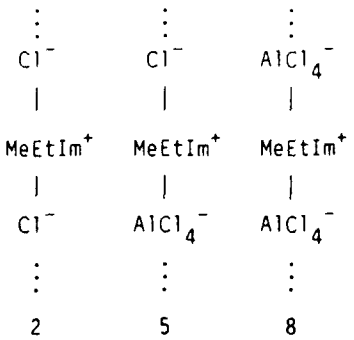

Figure 7. Cation environments.

Equation 8 may be restated in terms of Y_4 to give

$$\delta_{obs} = \delta_2 + (2\delta_5 - 2\delta_2)Y_4 + (\delta_8 - 2\delta_5 + \delta_2)Y_4^2 \qquad (9)$$

A simple ion pairing model would be linear in Y_4. Figure 8 shows some ^1H and ^{13}C data for the entire basic composition range in the $AlCl_3$-MeEtImCl melts. The solid lines are calculated from equation 9 and the dashed lines are for the linear ion pairing model.

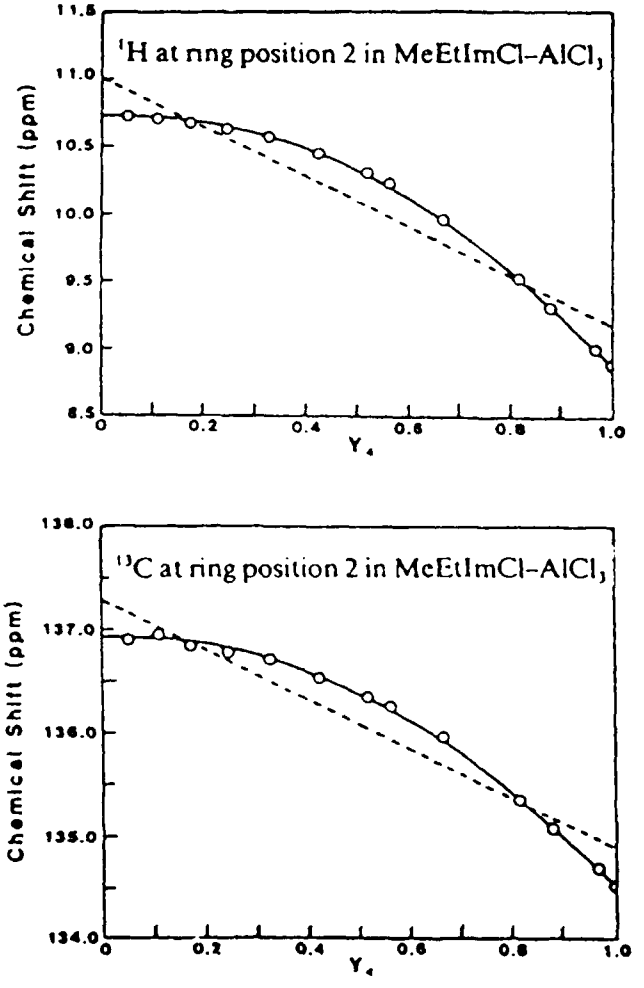

Figure 8. NMR in $AlCl_3$-MeEtImCl melts.

Melt compositions with the highest proportion of Cl^- anions (i.e., the most basic) have chemical shifts that are the most deshielded. This is reasonable, since Cl^- is more polarizing than $AlCl_4^-$ and one would expect a greater effect on the $MeEtIm^+$ cation.

The addition of a solvent, such as acetonitrile or benzene, to a basic melt has the same effect as removing Cl^-. Again, this is reasonable due to the mitigation of the interaction between Cl^- and $MeEtIm^+$ by solvation.

3.1.3 Complexation. There is a large body of electrochemical evidence that shows that metal ions are complexed in the room temperature chloroaluminate molten salts. NMR can be used to determine some details about the complexes formed in the melts. Figure 9 shows that when a metal ion is added to a basic $AlCl_3$-MeEtImCl melt, it affects the chemical shift of the $MeEtIm^+$ cation. The direction of the change in chemical shifts is as if the metal ion was removing Cl^- from the melt. The magnitude of the shift change for a given amount of added metal ion may predicted from the model

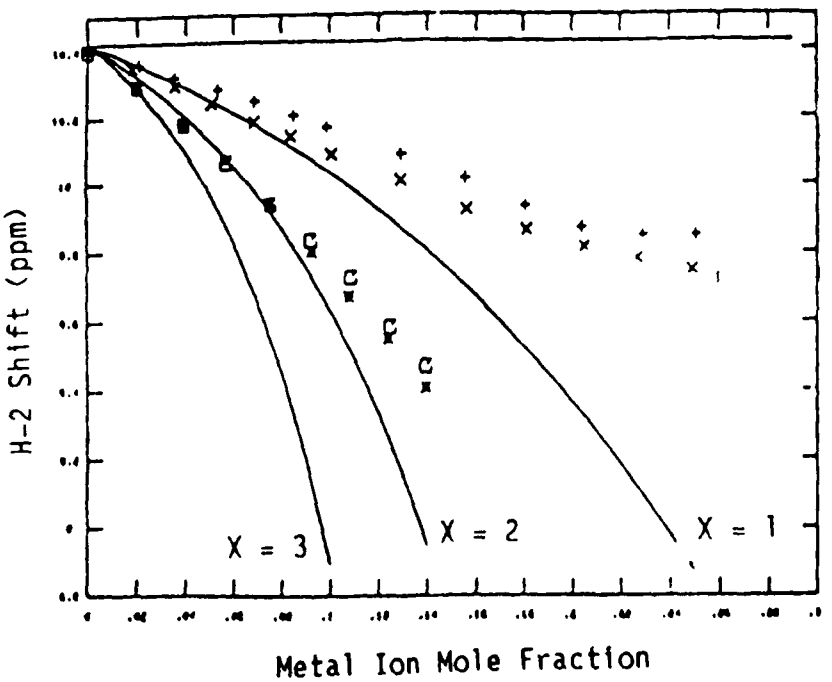

Figure 9. Addition of metal ion chlorides to basic $AlCl_3$-MeEtImCl melt. +=LiCl, X=AgCl, *=$CdCl_2$, □=$ZnCl_2$.

described by Equation 8 (solid lines in figure 9). The effect of the metal ion will depend primarily on the number of Cl^- (x) consumed by metal ion M^+ in forming the complex

$$MCl_y + xCl^- \rightleftarrows MCl_{x+y}^{x-}.$$

At low concentrations of added metal ion the measured chemical shifts are as predicted for dichloro (for Li^+ and Ag^+) or tetrachloro (Cd^{2+} and Zn^{2+}) complexes. The deviations from predicted shifts at higher metal ion concentrations is almost certainly due to the fact that the metal ion complex will itself affect the chemical shifts of the $MeEtIm^+$. A more complex model shown in figure 10 is required to predict the shifts in the ternary melts.

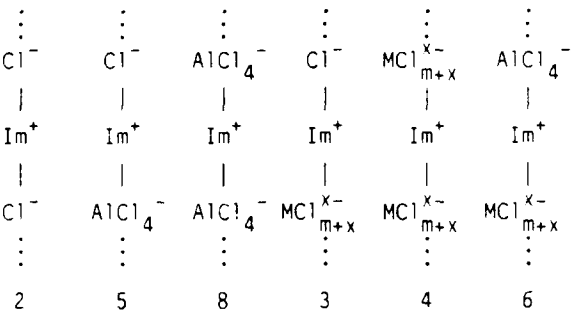

Figure 10. Melt model for ternary melts.

The model in figure 10 results in Equation 10:

$$\delta_{obs} = Y_4^2(\delta_2-2\delta_5+\delta_8) + Y_4(2\delta_5-2\delta_2) + \delta_2 + Y_4Y_M(2\delta_6-2\delta_3+2\delta_2-2\delta_5) + Y_M(2\delta_3-2\delta_2) + Y_M^2(\delta_2+\delta_4-2\delta_3) \quad (10)$$

Y_M is the ion fraction of the metal ion. The δ_i's are obtained by experiments in $AlCl_3$-MeEtImCl and $AlCl_3$-MCl_y binary melts and by curve fitting. Figure 11 shows how Equation 9 now fits the data for $AlCl_3$-MeEtImCl-LiCl ternaries.

^7Li NMR experiments in $AlCl_3$-BuPyCl-LiCl melts are also consistent with the formation of $LiCl_2^-$ (10).

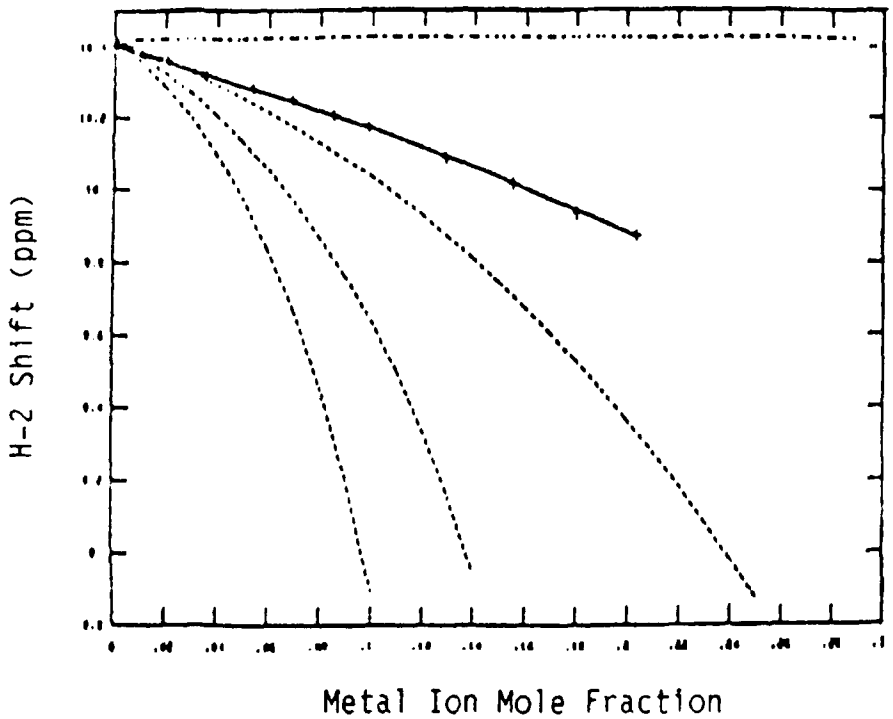

Figure 11. ^1H NMR at H-2 in $AlCl_3$-MeEtImCl-LiCl ternary melts. Solid line calculated by equation 9 for formation of $LiCl_2^-$.

3.2 Organic Halides

^1H NMR has been used by Angell and Shuppert to study the structure of molten pyridinium chloride (PyHCl)(11). In this melt hydrogen bonding is possible between the N-H of the pyridine ring and Cl^-. $AlCl_3$ was added to the PyHCl melt to form a series of low melting binary compositions. The chemical shifts of the ring protons were found to be sensitive to the mole fraction $AlCl_3$ in the binaries, with a sharp change at about the 1:2 $AlCl_3$:PyHCl composition. The phase diagram indicated compound formation at that composition. The data indicate that the PyHCl melt exists as $(PyH\cdots Cl\cdots HPy)^+Cl^-$, and that $AlCl_3$ complexes first with the free Cl^- then the hydrogen bonded Cl^- as more $AlCl_3$ is added to a binary melt. An estimate of the equilibrium constant for

$$2PyH^+ + Cl^- \rightleftarrows (PyH\cdots Cl\cdots HPy)^+$$

was made by using the NMR data to determine the equilibrium amounts of the PyH^+ species. Chemical exchange at the fast exchange limit was assumed and the chemical shifts were fitted to a two site exchange model.

A series of molten methylpyridinium halides has been studied by Newman and coworkers (12). The proton chemical shifts indicated the presence and absence of hydrogen bonding in various examples of the melts. The authors were able to correlate the NMR behavior with transport properties.

3.3 Inorganic Halides

Hafner and Nachtrieb describe the use of ^{205}Tl NMR to determine the nature of the interactions between cations and chloride and nitrate anions in Tl containing melts (13). The chemical shifts of thalium ions are extremely sensitive to short range interactions due to a high receptivity and the fact that the outer shell electrons are 6s, and thus easily deformable. The chemical shift for thallous salts can be more than 10^4 ppm. Nakamura et al. have extended the earlier work in recent years (14). By relating the observed chemical shifts to fundamental chemical shift theory (see Equation 4), the authors have determined cation-anion distances and directly probed the degree of covalency in thallous halides. In binary thallium halide-alkali halide melts, the effect of the alkali metal cation on the Tl^+-X^- and Tl^+-NO_3^- overlap was revealed. The chemical shifts implied significant covalent character in some of these melts.

4. REFERENCES

1. High Resolution NMR - Theory and Chemical Applications, E. D. Becker, Academic Press, 1980.

2. Nuclear Magnetic Resonance Spectroscopy, R. K. Harris, Pitman Books Ltd., 1983.

3. J. Gray and G. Maciel, J. Am. Chem. Soc., **103**, 7147 (1981).

4. J. S. Wilkes, G. F. Reynolds and J. S. Frye, Inorg. Chem., **22**, 3870 (1983).

5. L. P. Davis, C. J. Dymek, J. J. P. Stewart, H. J. Clark and W. J. Lauderdale, J. Am. Chem. Soc., **107**, 5041 (1985).

6. T. Matsumoto and K. Ichikawa, J. Am. Chem. Soc., **106**, 4316 (1984).

7. L. Dalton and J. Wilkes, unpublished results.

8. J. Wilkes, unpublished results.

9. J. Robinson, R. C. Bugle, H. L. Chum, D. Koran, and R. A. Osteryoung, J. Am. Chem. Soc., **101**, 3776 (1979).

10. F. Taulelle and A. I. Popov, Polyhedron, 889 (1983).

11. C. A. Angell and J. W. Shuppert, J. Phys. Chem., **84**, 538 (1980).

12. D. Newman, R. Rhinebarger, D. Siconolfi and O. Banjoko, J. Electrochem. Soc., **128**, 2331 (1981).

13. S. Hafner and N. Nachtrieb, J. Chem. Phys., **40**, 2891 (1964).

14. Y. Nakamura, Y. Kitazawa, M. Shimoji and S. Shimokawa, J. Phys. Chem., **87**, 5117 (1983).